

On Overcoming the Transverse Boundary Error of the SU/PG Scheme for Moving Conductor Problems

Sethupathy Subramanian[†], Udaya Kumar,[‡] *Senior Member, IEEE* and Sujata Bhowmick^{*}

[†]Department of Physics, University of Notre Dame, IN 46556, USA

[‡]Department of Electrical Engineering, ^{*}Department of Electronic Systems Engineering,
Indian Institute of Science, Bangalore 560012, India

Conductor moving in magnetic field is quite common in electrical equipment. The numerical simulation of such problem is vital in their design and analysis of electrical equipment. The Galerkin finite element method (GFEM) is a commonly employed simulation tool, nonetheless, due to its inherent numerical instability at higher velocities, the GFEM requires upwinding techniques to handle moving conductor problems. The Streamline Upwinding/Petrov-Galerkin (SU/PG) scheme is a widely acknowledged upwinding technique, despite its error-peaking at the transverse boundary. This error at the transverse-boundary, is found to be leading to non-physical solutions. Several remedies have been suggested in the allied fluid dynamics literature, which employs non-linear, iterative techniques. The present work attempts to address this issue, by retaining the computational efficiency of the GFEM. By suitable analysis, it is shown that the source of the problem can be attributed to the Coulomb's gauge. Therefore, to solve the problem, the Coulomb's gauge is taken out from the formulation and the associated weak form is derived. The effectiveness of this technique is demonstrated with pertinent numerical results.

Index Terms—Numerical stability, Galerkin finite element method, Streamline upwinding/Petrov-Galerkin scheme, Transverse boundary error

I. INTRODUCTION

THE moving conductor problems are the class of problems, involving conductor moving in a magnetic field (\mathbf{B}_a). As a consequence, there would be an induced current (\mathbf{J}) in the conductor, which in turn produces a reaction magnetic field (\mathbf{b}). The quantification of the reaction magnetic field and the associated induced currents, are vital for the design and analysis of the electrical equipment such as electromagnetic flowmeter, linear induction motor, eddy current brakes etc. For the ease of further discussion, the governing equations of the moving conductor problem are enumerated below [1], [2],

$$\sigma \nabla \phi - \left(\nabla \cdot \frac{1}{\mu} \nabla \right) \mathbf{A} - \sigma \mathbf{u} \times \nabla \times \mathbf{A} = \sigma \mathbf{u} \times \mathbf{B}_a \quad (1)$$

$$\nabla \cdot (\sigma \nabla \phi) - \nabla \cdot (\sigma \mathbf{u} \times \nabla \times \mathbf{A}) = \nabla \cdot (\sigma \mathbf{u} \times \mathbf{B}_a) \quad (2)$$

where, ϕ is the scalar potential arising out of the current flow, \mathbf{A} is the magnetic vector potential associated with reaction magnetic field \mathbf{b} , \mathbf{u} is the velocity of the moving conductor, μ is the magnetic permeability and σ is the electrical conductivity.

Owing to the coupled nature as well as the vectorial form of the governing equations, finding an analytical solution is nearly impossible and hence, numerical simulation is the only choice available. Among the available numerical schemes, the Galerkin finite element method (GFEM) is widely employed for the simulation in different disciplines of engineering including electrical engineering. Despite its widespread success, as the velocities become higher the GFEM results suffer

from numerical oscillations [3]–[6]. Specifically, when the element Peclet number $Pe = \mu \sigma \|\mathbf{u}\| \Delta l / 2 > 1$ (Δl is the element length along the direction of the velocity), the numerical oscillations appears in the solution. This issue is comprehensively discussed in the allied literature and several remedies have been suggested [3].

The upwinding schemes are the earliest and popular ones suggested in the fluid dynamics literature and these have been extensively adopted in the moving conductor literature as well [7]–[17]. It can be worth noting here that the occurrence of numerical oscillations at higher velocities is common to many numerical schemes including the edge element method and there are few upwinding remedies suggested in the literature [18], [19]. Owing to the presence of substantial cross-research, the upwinding schemes of nodal elements are well studied and well established. Hence, the present work employs nodal finite elements for the study. Among the nodal upwinding schemes, the Streamline upwinding/Petrov Galerkin (SU/PG) scheme is the latest and the widely adopted one. Though, the SU/PG scheme successfully removes the numerical oscillations, there are numerous instances wherein, it leads to error at the transverse boundary [20]. This problem is scarcely discussed in the electrical engineering literature, except for a recent effort in which the existence of such an error is pointed out for moving conductor problems [21]. Further, it is also shown that this in turn leads to non-physical currents in the adjacent air region.

In order to address this issue, several approaches have been suggested in fluid dynamics literature [20], [22], [23], which are termed as, 'Spurious Oscillations at Layers Diminishing (SOLD) methods' [24], [25]. These schemes being non-linear involve an iterative calculation procedure, which is a computationally time consuming process. Moreover, the implementation of SOLD schemes for electrical engineering

problems can be rarely seen in the literature. In any case, a recent work has shown that SOLD schemes are not fully free from boundary error [25]. The present work aims to investigate the origin of this error and perhaps suggest a solution.

Given these, the present work aims to investigate on the genesis of this boundary error in the SU/PG formulation for the moving conductor problem. It further aims to provide a simple and computationally efficient route to eliminate this error for moving conductor problems.

II. PRESENT WORK

A. Analysis with 2D version of the problem

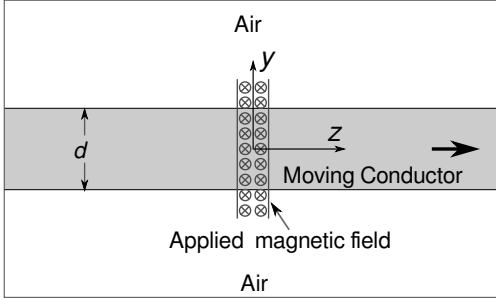


Fig. 1. Schematic of the 2D problem.

In reference [21], 2D version of the moving conductor problem, which has adequate representation of the 3D problem, has been considered for evaluating the error at the interface. For the sake of completeness, a brief description of the 2D problem is provided here (see Fig. 1). An infinite conducting slab with thickness d is placed between two air layers of thickness $4d$. The conductor has a uniform velocity u_z along the z -axis and a localized x -directed magnetic field is considered. Boundary in the flow direction is introduced at $20d$ on either side of the magnetic field. The material properties of the slab are $\sigma = 7.21 \times 10^6 \text{ Sm}^{-1}$, $\mu_r = 1$, $d = 0.5\text{m}$. The FEM discretisation involved 5760 nodal, bilinear quadrilateral elements of rectangular shape. The element size is varied along the y -direction to accurately capture the currents circulating in the conductor. It can be noted that the 2D problem here represents the circulation of current and thus it consists of 2-components of vector potential A_y, A_z .

The same 2D problem will be considered here for further analysis. In [21], it is shown that only SU/PG scheme suffers from boundary error and not the original Galerkin scheme or its variants [26]. In order to trace the genesis of this error numerically, computed results are analysed to detect the presence of any inconsistency.

During the analysis, it is found that the use of Coulomb's gauge i.e., $\nabla \cdot \mathbf{A} = 0$ condition, is being grossly violated in the SU/PG scheme, which is not the case with the GFEM based schemes. As an example, a sample result of $\nabla \cdot \mathbf{A}$ computed from the SU/PG scheme is presented in the Fig. 2a, where the presence of error could be clearly seen. Recently, a simple alternative scheme which is based on the classical GFEM has been presented in [26] and it is shown to be very stable. The computed $\nabla \cdot \mathbf{A}$ obtained by employing this scheme is also presented, in Fig. 2b.

In order to make a meaningful assessment, for each of the Pe , peak values of the b_x is taken for normalisation. The required values are taken from the results presented in [21], which has been reproduced as Fig. 3c for a ready reference. By comparing the results, it can be seen that the value of error in $\nabla \cdot \mathbf{A}$ is about 30% in the SU/PG solution, while it is only about 5% for the scheme proposed in [26]. This suggests a method for a direct correlation between the transverse boundary error and the peak magnitude of $\nabla \cdot \mathbf{A}$. To get a more quantitative picture, both the peak error as well as the peak $\nabla \cdot \mathbf{A}$ are obtained for a range of Pe and plotted in Figs. 2c and 2d. It is clear that the peak values of $\nabla \cdot \mathbf{A}$ and the peak boundary error with SU/PG scheme follows the exact same trend over the range of Pe .

This exercise clearly indicate that the boundary error in the solution is strongly correlated with the existence of $\nabla \cdot \mathbf{A} = 0$ in the weak solution through SU/PG scheme. It is worth noting here that the Coulombs gauge is commonly employed in moving conductor literature [7], [11]–[13], [27] especially for the nodal formulation. The following vector identity is employed most of the times,

$$\nabla \times \nabla \times \mathbf{A} = \nabla(\nabla \cdot \mathbf{A}) - \nabla^2 \mathbf{A} \quad (3)$$

assuming $\nabla \cdot \mathbf{A} = 0$,

$$\nabla \times \nabla \times \mathbf{A} = -\nabla^2 \mathbf{A} \quad (4)$$

However, the results of SU/PG scheme does not confirm to $\nabla \cdot \mathbf{A} = 0$ and therefore, it is necessary to avoid the use of Coulomb's gauge (refer to Figs. 2a & 2c). For this the corresponding term must be retained in the formulation. Please note that this might result in non-unique value of \mathbf{A} , however, it is $\nabla \times \mathbf{A}$ is the variable of interest not \mathbf{A} directly.

As the weak form for the Ampere's law (which involves $\nabla \times \nabla \times \mathbf{A}$) is not readily available for scalar elements, it will be dealt below.

The weighted residue formulation for the x -component of $\nabla \times \frac{1}{\mu} \nabla \times \mathbf{A}$ is,

$$\int_{\Omega} N_g (\nabla \times \frac{1}{\mu} \nabla \times \mathbf{A}) \cdot \hat{\mathbf{x}} d\Omega \quad (5)$$

where N_g is the Galerkin weighting function and $\hat{\mathbf{x}}$ is the unit vector along the x -axis. Applying the vector identity given in (3) on (5),

$$\Rightarrow \int_{\Omega} N_g \nabla \cdot \left(\frac{1}{\mu} \frac{\partial \mathbf{A}}{\partial x} - \frac{1}{\mu} \nabla A_x \right) d\Omega \quad (6)$$

Applying integration by parts for (6),

$$\begin{aligned} \Rightarrow & - \int_{\Omega} \nabla N_g \cdot \left(\frac{1}{\mu} \frac{\partial \mathbf{A}}{\partial x} - \frac{1}{\mu} \nabla A_x \right) d\Omega \dots \\ & + \oint_{\Gamma} N_g \left(\frac{1}{\mu} \frac{\partial \mathbf{A}}{\partial x} - \frac{1}{\mu} \nabla A_x \right) \cdot \hat{\mathbf{n}} d\Gamma \end{aligned} \quad (7)$$

where, $\hat{\mathbf{n}}$ is the unit normal vector. Remember that in the Laplacian formulation of scalar potential, by neglecting the boundary integral term in the weak form, the inter element boundary condition $\mathbf{D}_1 \cdot \hat{\mathbf{n}} = \mathbf{D}_2 \cdot \hat{\mathbf{n}}$ or $\mathbf{J}_1 \cdot \hat{\mathbf{n}} = \mathbf{J}_2 \cdot \hat{\mathbf{n}}$ get automatically satisfied [28]. Thus, it was not necessary

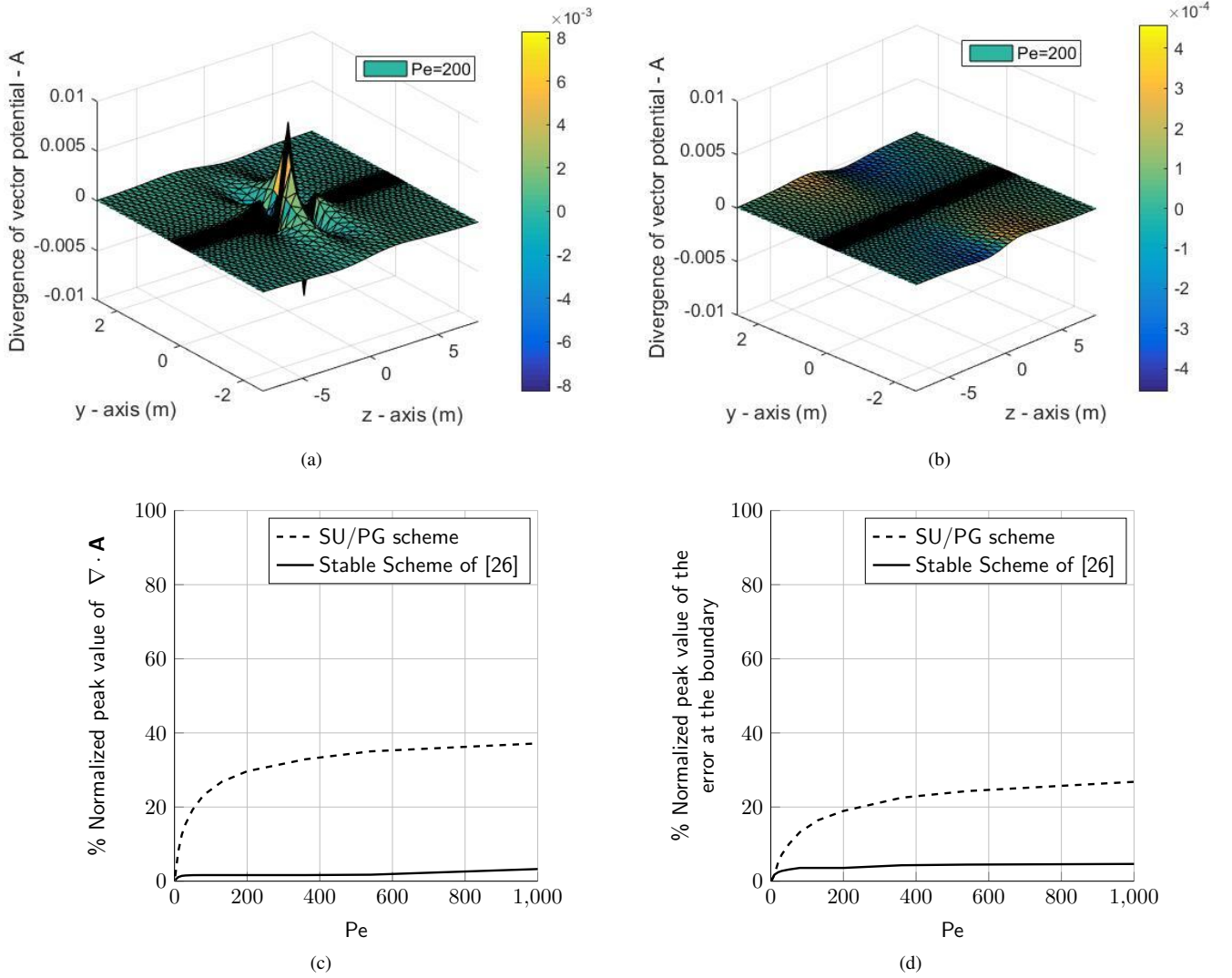


Fig. 2. Selected results from the 2D problem. (a) $\nabla \cdot \mathbf{A}$ obtained from the SU/PG scheme (b) $\nabla \cdot \mathbf{A}$ obtained from Scheme presented in [26] (c) Peak values $\nabla \cdot \mathbf{A}$ over a range of Pe obtained from SU/PG scheme and the stable scheme reported in [26]. (d) Peak values of the error over a range of Pe as obtained from SU/PG scheme and the stable scheme reported in [26].

to compute the boundary integral term there and that greatly improved the computational efficiency. Considering this, it is worthwhile to see the effect of neglecting the boundary integral term in the equation (7). The boundary integral term can be simplified as follows,

$$\begin{aligned}
 &\Rightarrow \oint_{\Gamma} N_g \left(\frac{1}{\mu} \frac{\partial \mathbf{A}}{\partial x} - \frac{1}{\mu} \nabla A_x \right) \cdot \hat{\mathbf{n}} \, d\Gamma \\
 &= \oint_{\Gamma} \frac{N_g}{\mu} \left(\frac{\partial A_y}{\partial x} n_y + \frac{\partial A_z}{\partial x} n_z - \frac{\partial A_x}{\partial y} n_y - \frac{\partial A_x}{\partial z} n_z \right) d\Gamma \\
 &= \oint_{\Gamma} N_g (h_z n_y - h_y n_z) \, d\Gamma
 \end{aligned} \tag{8}$$

where,

$$h_z = \frac{1}{\mu} \left(\frac{\partial A_y}{\partial x} - \frac{\partial A_x}{\partial y} \right) \quad \text{and} \quad h_y = \frac{1}{\mu} \left(\frac{\partial A_x}{\partial z} - \frac{\partial A_z}{\partial x} \right)$$

Equation (8) corresponds to the x -component, the boundary integral terms for other components can also be derived in the same fashion. The boundary integral term for the y -component is,

$$\oint_{\Gamma} N_g (h_x n_z - h_z n_x) \, d\Gamma \tag{9}$$

and that for the z -component is,

$$\oint_{\Gamma} N_g (h_y n_x - h_x n_y) \, d\Gamma \tag{10}$$

Combining (8), (9) and (10), the vector form of the boundary integral terms can be written as,

$$\Rightarrow - \oint_{\Gamma} N_g (\mathbf{h} \times \mathbf{n}) \, d\Gamma \tag{11}$$

Equating (11) to zero results in maintaining the tangential continuity of the magnetic field intensity \mathbf{h} [29], i.e.,

$$\mathbf{h}_1 \cdot \hat{\mathbf{t}} \approx \mathbf{h}_2 \cdot \hat{\mathbf{t}} \tag{12}$$

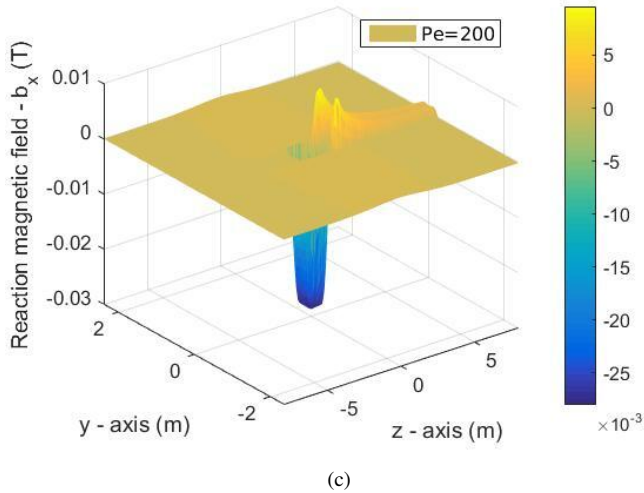
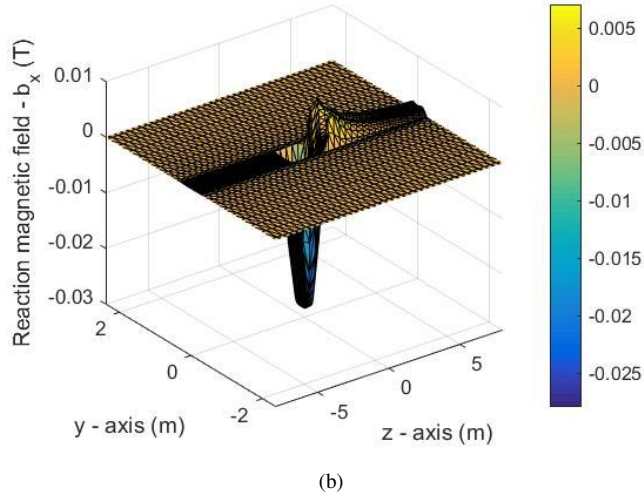
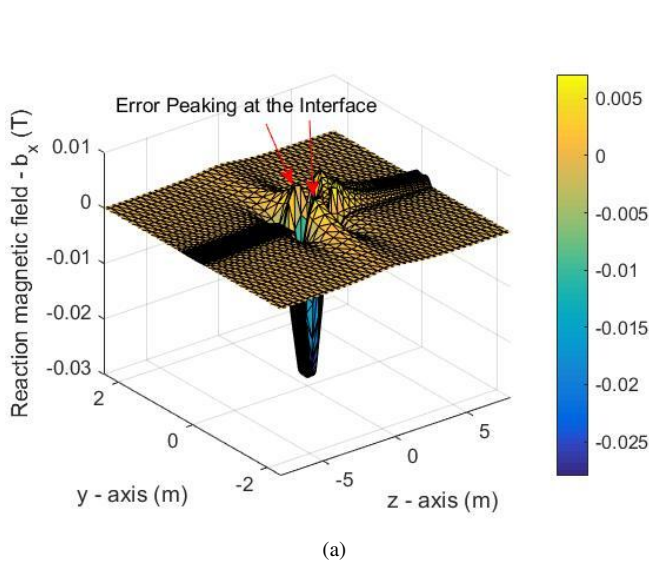


Fig. 3. Reaction magnetic field b_x obtained with the SU/PG scheme for $Pe = 200$. (a) With the assumption of $\nabla \cdot \mathbf{A} = 0$ (b) Without the assumption of $\nabla \cdot \mathbf{A} = 0$ (c) Reference solution generated with very fine discretisation [21]

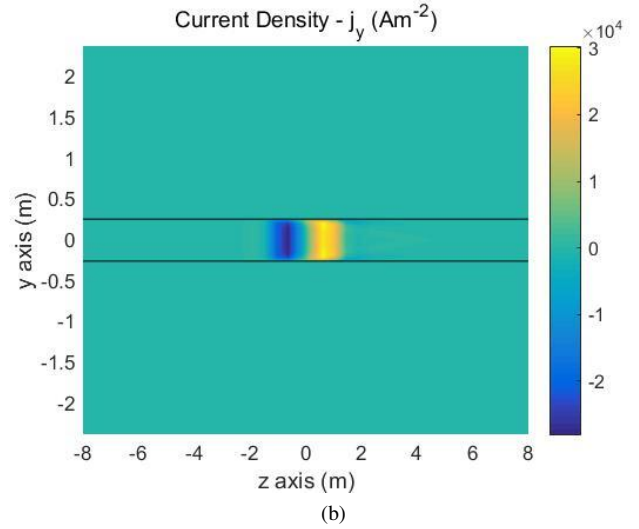
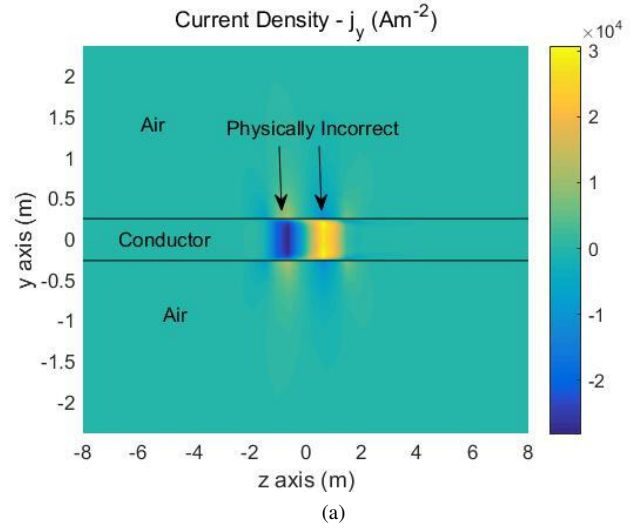


Fig. 4. Current density $j_y = \partial h_x / \partial z$, obtained with the SU/PG scheme for $Pe = 200$. (a) With the assumption of $\nabla \cdot \mathbf{A} = 0$ (b) Without the assumption of $\nabla \cdot \mathbf{A} = 0$

across the elements 1 and 2. Thus, neglecting the boundary integral in (7), helps to maintain the continuity of magnetic field intensity across the element interface. Therefore, the weak formulation contains only the volume integral term in the proposed approach and the complete SU/PG-weak formulation of (1) and (2) are provided in the Appendix A.

With this, the simulations are carried out for range of Peclet numbers and the sample simulation results are presented in Fig. 3. When the $\nabla \cdot \mathbf{A}$ is retained with the SU/PG scheme, error at the transverse boundary virtually disappears. Also, It can be clearly seen that the reaction magnetic field profile obtained with the proposed approach (Fig. 3b) is matching exactly with the reference solution presented in Fig. 3c. Consequently, the non-physical solution of $\nabla \times \mathbf{h} \neq 0$ in the adjacent air-region, is also seem to be practically absent with the proposed approach (refer to Fig. 4, which provides solution for both). For a range of Pe considered in Fig. 2c, the simulation results with $\nabla \cdot \mathbf{A}$ retained is found to have

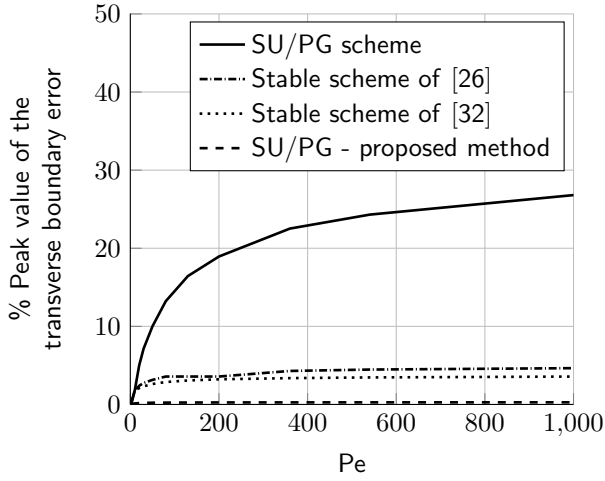


Fig. 5. Comparison of % peak value of transverse boundary error present in different schemes

peak error $< 1\%$ (refer to Fig 5). In the next subsection, the effect of avoiding Coulomb's gauge on the condition number of the FEM matrix is discussed.

B. Effect on condition number

It is evident that the avoiding Coulomb's gauge from the governing equation can impact the condition number of the final FEM matrix. In order to address this, a possible remedy is discussed in this subsection. In this, a scaled amount of $\nabla \cdot \mathbf{A}$ is injected into the original governing equation, with the scaling parameter α . The results of this new variation is tabulated in Table I. For comparison, simulations also carried using the edge elements and the results of same is included in Table I. As mentioned in the introduction, the edge elements cannot inherently avoid the erroneous results arising out of the convection dominated simulations.

As shown in the table I, the % peak error in the proposed scheme can be seen to slowly increase as we increase the $\nabla \cdot \mathbf{A}$ contribution. However, for the values of α listed in the table, the accuracy of the proposed scheme is substantially better than the edge element method or the SU/PG scheme. When $\alpha = 0.05$ or in other words, when the $\nabla \cdot \mathbf{A}$ addition is around 5%, the accuracy at the material interface is at least an order of magnitude better than the other methods; while keeping the condition number in a comparably reasonable value.

It can also be observed that the condition number from the edge element method is not better than the nodal element method. This may be attributed to the absence of normal continuity across the edge elements [30], [31].

C. Verification with 3D electromagnetic flowmeter problem

As a demonstration of the efficacy of the proposed approach in real life situations, a practical 3D problem, the electromagnetic flowmeter, is simulated for high Peclet numbers. The simulation is carried out using the bilinear nodal elements. The simulation parameters and the input quantities are taken as mentioned in [26] and the schematic diagram of the electromagnetic flowmeter is shown in Fig. 6, with its x, y, z -axes

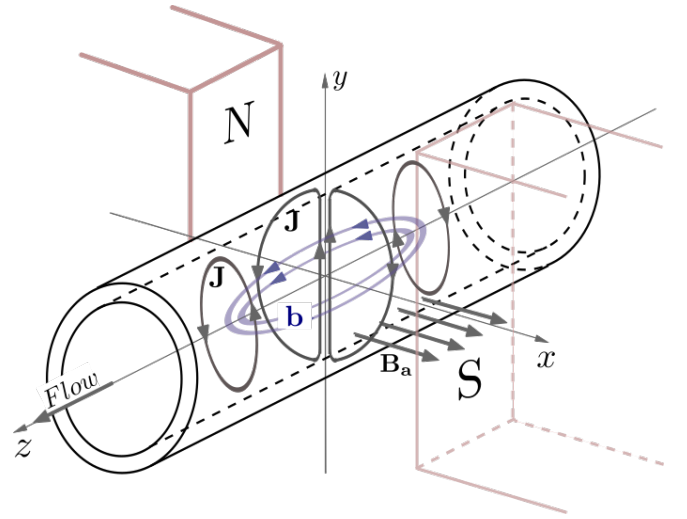


Fig. 6. Schematic of the electromagnetic flowmeter, shown with the current density \mathbf{J} and the reaction magnetic field \mathbf{b}

defined. The simulations are carried out for a range of Peclet numbers and the results are confirming the conclusions, which are drawn for the 2D problem. The sample simulation results are presented in Fig. 7, with $Pe = 1600$. From Fig. 7a the non-physical current distribution in the air region can be seen, which is obtained from the SU/PG scheme, on the other hand, the retention of $\nabla \cdot \mathbf{A}$ in the SU/PG scheme provides a physically confirming solution (refer to Fig. 7b).

Incidentally, the recent pole-zero cancellation based, stabilization schemes proposed in [26], [32] observed to give accurate solutions without the boundary error. A sample simulation result for $Pe = 1600$ with the scheme proposed in [32], is provided in Fig. 8.

Referring to Fig. 6, along the zy -plane the complete circulation of induced current is represented. In the orthogonal direction, i.e., along the zx -plane the currents are orthogonal to the plane and they are mostly represented by the y -component of the current density j_y . The currents along the zx -plane does not get directly oriented by the boundary, unlike the circulation along the zy -plane. Owing to this, the boundary error is expected to be minimal along the zx -plane and the same is observed with this 3D simulation. To confirm this observation further, the 2D version of the moving conductor problem along the zx -plane is simulated. The results from this simulation indicate insignificant boundary error, along the zx -plane.

III. SUMMARY AND CONCLUSION

The SU/PG scheme is widely adopted upwinding technique, for high flow velocity problems due to its simplicity and being void of crosswind of diffusion [33]. Besides, the transverse boundary error present in the SU/PG scheme is a serious issue and several non-linear solutions have been proposed (called as SOLD schemes) by the computational fluid dynamics community. Nevertheless, they suffer from computational inefficiency, as well as, some inaccuracy [24], [25]. In addition, these techniques are rarely employed for moving conductor problems.

TABLE I
COMPARISON OF CONDITION NUMBER AND ACCURACY

Pe	SU/PG scheme with Proposed method (Node element)			Edge Element		SUPG Scheme (Node element)	
	α	Condition no.	% Peak Error	Condition no.	% Peak Error	Condition no.	% Peak Error
50	0.00	8.9415e+11	0.221	4.8747e+09	22.516	1.7352e+08	10.007
	0.05	4.1364e+08	2.215				
	0.10	3.2260e+08	3.466				
200	0.00	1.5178e+12	0.257	1.9438e+10	25.018	1.8165e+09	18.942
	0.05	2.0991e+09	3.359				
	0.10	1.9721e+09	5.361				
1000	0.00	2.1925e+14	0.271	3.3003e+11	25.733	1.8677e+11	30.021
	0.05	4.0514e+11	4.289				
	0.10	3.4614e+11	6.791				

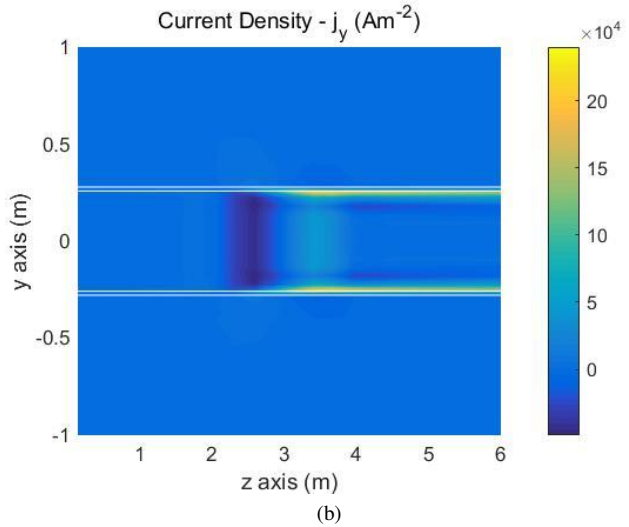
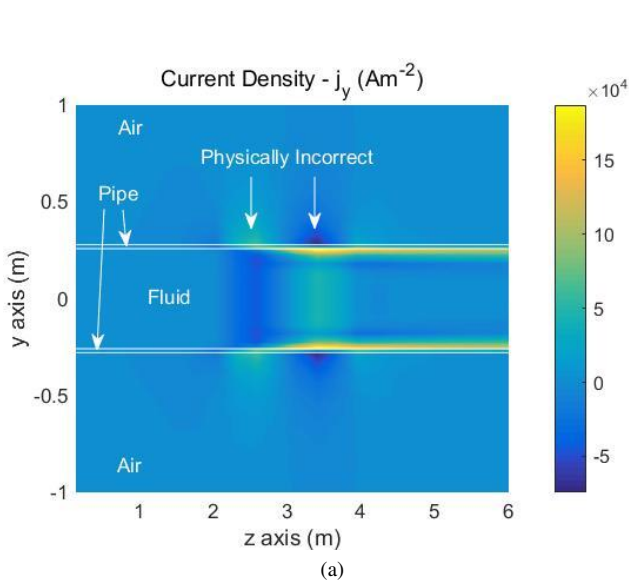


Fig. 7. Current density $j_y = \partial h_x / \partial z - \partial h_z / \partial x$ in $x = 0$ plane, obtained with the SU/PG scheme for $Pe = 1600$. (a) With the assumption of $\nabla \cdot \mathbf{A} = 0$ (b) Without the assumption of $\nabla \cdot \mathbf{A} = 0$

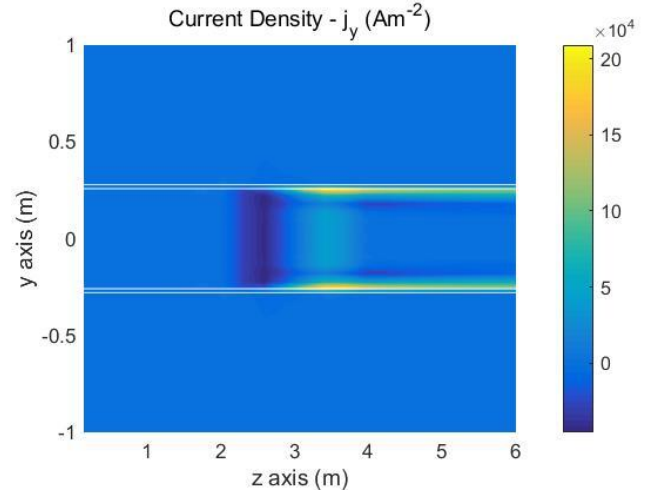


Fig. 8. Current density $j_y = \partial h_x / \partial z - \partial h_z / \partial x$ in $x = 0$ plane, obtained with the pole-zero cancellation based scheme [32] for $Pe = 1600$.

In the present work, a 2D version of the moving conductor problem, is taken for the analysis. The 2D problem represents the complete circulation of current with in the conducting region and thus it consists of 2-components of vector potential. Here, the source of the transverse boundary error is identified with the enforcement of Coulomb gauge $\nabla \cdot \mathbf{A} = 0$. Therefore, the $\nabla \cdot \mathbf{A}$ term is retained and the weak form of the Amperes' law has been derived for scalar elements. Then, through the numerical simulation of 2D, as well as, 3D problems, it is shown that the retention of $\nabla \cdot \mathbf{A}$ practically eliminates the material interface boundary error present in the SU/PG scheme. In addition, this approach preserves the linearity, as well as, computational efficiency of the SU/PG scheme.

APPENDIX A WEAK FORM OF THE GOVERNING EQUATIONS

The weak form of (2) can be commonly found in the computational electromagnetic literature. Nevertheless, for the sake of completeness and quick reference, it has been provided

below, along with the weak form of (1), which is derived. The weak form of (2) can be written as,

$$\begin{aligned} \int_{\Omega} \sigma \nabla N_g \cdot \nabla \phi \, d\Omega - \int_{\Omega} \sigma \nabla N_g \cdot (\mathbf{u} \times \nabla \times \mathbf{A}) \, d\Omega \dots \\ = \int_{\Omega} \sigma \nabla N_g \cdot (\mathbf{u} \times \mathbf{B}_a) \, d\Omega \end{aligned} \quad (13)$$

The advection-diffusion form of (1) requires the modification of the Galerkin weighting function N_g to the SU/PG weighting function N_s , which is given by,

$$N_s = N_g + \tau \frac{\Delta l}{2\|\mathbf{u}\|} \cdot \nabla N_g \quad (14)$$

where τ is the stabilization parameter, defined as $\tau \equiv \coth(|Pe|) - 1/|Pe|$. The stabilization parameter τ decides the optimal (right) amount of upwinding which is being added to the Galerkin weight function N_g . This added term, is employed to only the element interiors and in case of linear elements, the second derivative vanishes and the modified weighting function N_s is applied only to the advective/first derivative terms [33]–[35]. Therefore, the weak form of the x -component of (1) takes the form:

$$\begin{aligned} \int_{\Omega} \sigma N_s \frac{\partial \phi}{\partial x} \, d\Omega - \int_{\Omega} \nabla N_g \cdot \left(\frac{1}{\mu} \frac{\partial \mathbf{A}}{\partial x} - \frac{1}{\mu} \nabla A_x \right) \, d\Omega \dots \\ - \int_{\Omega} \sigma N_s \left(u_y \frac{\partial A_y}{\partial x} - u_y \frac{\partial A_x}{\partial y} - u_z \frac{\partial A_x}{\partial z} + u_z \frac{\partial A_z}{\partial x} \right) \, d\Omega \dots \\ + \alpha \int_{\Omega} \frac{\partial N_g}{\partial x} \nabla \cdot \mathbf{A} \, d\Omega = \int_{\Omega} \sigma N_s (u_y B_z - u_z B_y) \, d\Omega \end{aligned} \quad (15)$$

and its y -component:

$$\begin{aligned} \int_{\Omega} \sigma N_s \frac{\partial \phi}{\partial y} \, d\Omega - \int_{\Omega} \nabla N_g \cdot \left(\frac{1}{\mu} \frac{\partial \mathbf{A}}{\partial y} - \frac{1}{\mu} \nabla A_y \right) \, d\Omega \dots \\ - \int_{\Omega} \sigma N_s \left(u_z \frac{\partial A_z}{\partial y} - u_z \frac{\partial A_y}{\partial z} - u_x \frac{\partial A_y}{\partial x} + u_x \frac{\partial A_x}{\partial y} \right) \, d\Omega \dots \\ + \alpha \int_{\Omega} \frac{\partial N_g}{\partial y} \nabla \cdot \mathbf{A} \, d\Omega = \int_{\Omega} \sigma N_s (u_z B_x - u_x B_z) \, d\Omega \end{aligned} \quad (16)$$

and its z -component:

$$\begin{aligned} \int_{\Omega} \sigma N_s \frac{\partial \phi}{\partial z} \, d\Omega - \int_{\Omega} \nabla N_g \cdot \left(\frac{1}{\mu} \frac{\partial \mathbf{A}}{\partial z} - \frac{1}{\mu} \nabla A_z \right) \, d\Omega \dots \\ - \int_{\Omega} \sigma N_s \left(u_x \frac{\partial A_x}{\partial z} - u_x \frac{\partial A_z}{\partial x} - u_y \frac{\partial A_z}{\partial y} + u_y \frac{\partial A_y}{\partial z} \right) \, d\Omega \dots \\ + \alpha \int_{\Omega} \frac{\partial N_g}{\partial z} \nabla \cdot \mathbf{A} \, d\Omega = \int_{\Omega} \sigma N_s (u_x B_y - u_y B_x) \, d\Omega \end{aligned} \quad (17)$$

For the 2D problem considered, the x -component of the equation vanishes and only the y and z components remain. Also, the velocity is assumed to be along the z direction ($\mathbf{u} = u_z \hat{\mathbf{z}}$) and the input magnetic field is x directed ($\mathbf{B}_a = B_x \hat{\mathbf{x}}$).

With this, the weak forms of the governing equations (1) and (2) are respectively given by,

$$\begin{aligned} \int_{\Omega} \sigma N_s \frac{\partial \phi}{\partial y} \, d\Omega + \int_{\Omega} \frac{1}{\mu} \left(\frac{\partial N_g}{\partial z} \frac{\partial A_y}{\partial z} - \frac{\partial N_g}{\partial z} \frac{\partial A_z}{\partial y} \right) \, d\Omega \dots \\ + \int_{\Omega} \sigma N_s \left(u_z \frac{\partial A_y}{\partial z} - u_z \frac{\partial A_z}{\partial y} \right) \, d\Omega \dots \\ + \alpha \int_{\Omega} \frac{\partial N_g}{\partial y} \left(\frac{\partial A_y}{\partial y} + \frac{\partial A_z}{\partial z} \right) \, d\Omega = \int_{\Omega} \sigma N_s u_z B_x \, d\Omega \end{aligned} \quad (18)$$

$$\begin{aligned} \int_{\Omega} \sigma N_s \frac{\partial \phi}{\partial z} \, d\Omega + \int_{\Omega} \frac{1}{\mu} \left(\frac{\partial N_g}{\partial y} \frac{\partial A_z}{\partial y} - \frac{\partial N_g}{\partial y} \frac{\partial A_y}{\partial z} \right) \, d\Omega \dots \\ + \alpha \int_{\Omega} \frac{\partial N_g}{\partial z} \left(\frac{\partial A_y}{\partial y} + \frac{\partial A_z}{\partial z} \right) \, d\Omega = 0 \end{aligned} \quad (19)$$

$$\begin{aligned} \int_{\Omega} \sigma \left(\frac{\partial N_g}{\partial y} \frac{\partial \phi}{\partial y} + \frac{\partial N_g}{\partial z} \frac{\partial \phi}{\partial z} \right) \, d\Omega + \int_{\Omega} \sigma u_z \frac{\partial N_g}{\partial y} \frac{\partial A_y}{\partial z} \, d\Omega \dots \\ - \int_{\Omega} \sigma u_z \frac{\partial N_g}{\partial y} \frac{\partial A_z}{\partial y} \, d\Omega = \int_{\Omega} \sigma u_z B_x \frac{\partial N_g}{\partial y} \, d\Omega \end{aligned} \quad (20)$$

REFERENCES

- [1] O. Biro, K. Preis, W. Renhart, K. Richter, and G. Vrisk, "Performance of different vector potential formulations in solving multiply connected 3-d eddy current problems," *IEEE Trans. Magnetics*, vol. 26, no. 2, pp. 438–441, 1990.
- [2] T. Shimizu, N. Takeshima, and N. Jimbo, "A numerical study on faraday-type electromagnetic flowmeter in liquid metal system, (i)," *Journal of Nuclear Science and Technology*, vol. 37, no. 12, pp. 1038–1048, 2000.
- [3] O. Zienkiewicz, R. Taylor, and P. Nithiarasu, *The Finite Element Method for Fluid Dynamics*. Elsevier Science, 2005.
- [4] D. Spalding, "A novel finite difference formulation for differential expressions involving both first and second derivatives," *International Journal for Numerical Methods in Engineering*, vol. 4, no. 4, pp. 551–559, 1972.
- [5] A. Runchal, "Convergence and accuracy of three finite difference schemes for a two-dimensional conduction and convection problem," *International Journal for Numerical Methods in Engineering*, vol. 4, no. 4, pp. 541–550, 1972.
- [6] I. Christie, D. F. Griffiths, A. R. Mitchell, and O. C. Zienkiewicz, "Finite element methods for second order differential equations with significant first derivatives," *International Journal for Numerical Methods in Engineering*, vol. 10, no. 6, pp. 1389–1396, 1976.
- [7] M. Odamura, "Upwind finite element solution for saturated traveling magnetic field problems," *Electrical Engineering in Japan*, vol. 105, no. 4, pp. 126–132, 1985.
- [8] M. Ito, T. Takahashi, and M. Odamura, "Up-wind finite element solution of travelling magnetic field problems," *IEEE Trans. Magnetics*, vol. 28, no. 2, pp. 1605–1610, 1992.
- [9] D. Rodger, P. Leonard, and T. Karaguler, "An optimal formulation for 3d moving conductor eddy current problems with smooth rotors," *IEEE Trans. Magnetics*, vol. 26, no. 5, pp. 2359–2363, 1990.
- [10] E. Chan and S. Williamson, "Factors influencing the need for upwinding in two-dimensional field calculation," *IEEE Trans. Magnetics*, vol. 28, no. 2, pp. 1611–1614, 1992.
- [11] N. Allen, D. Rodger, P. Coles, S. Strret, and P. Leonard, "Towards increased speed computations in 3d moving eddy current finite element modelling," *IEEE Trans. Magnetics*, vol. 31, no. 6, pp. 3524–3526, 1995.
- [12] D. Rodger, T. Karguler, and P. Leonard, "A formulation for 3d moving conductor eddy current problems," *IEEE Trans. Magnetics*, vol. 25, no. 5, pp. 4147–4149, 1989.
- [13] J. Bird, T. Lipo *et al.*, "A 3-d magnetic charge finite-element model of an electrodynamic wheel," *IEEE Trans. Magnetics*, vol. 44, no. 2, pp. 253–265, 2008.

- [14] H. Vande Sande, H. De Gersem, and K. Hameyer, "Finite element stabilization techniques for convection-diffusion problems," *7th International journal of theoretical electrotechnics*, pp. 56–59, 1999.
- [15] L. Codecasa and P. Alotto, "2-d stabilized fit formulation for eddy-current problems in moving conductors," *IEEE Trans. Magnetics*, vol. 51, no. 3, pp. 1–4, 2015.
- [16] Y. Liang, "Steady-state thermal analysis of power cable systems in ducts using streamline-upwind/ Petrov-galerkin finite element method," *Dielectrics and Electrical Insulation, IEEE Transactions on*, vol. 19, no. 1, pp. 283–290, 2012.
- [17] S. Noguchi and S. Kim, "Magnetic field and fluid flow computation of plural kinds of magnetic particles for magnetic separation," *IEEE Trans. Magnetics*, vol. 48, no. 2, pp. 523–526, 2012.
- [18] E. X. Xu, J. Simkin, and S. C. Taylor, "Streamline upwinding in a 3-d edge-element method modeling eddy currents in moving conductors," *IEEE transactions on magnetics*, vol. 42, no. 4, pp. 667–670, 2006.
- [19] F. Henrotte, H. Heumann, E. Lange, and K. Hameyer, "Upwind 3-d vector potential formulation for electromagnetic braking simulations," *IEEE Transactions on Magnetics*, vol. 46, no. 8, pp. 2835–2838, 2010.
- [20] T. J. Hughes, M. Mallet, and M. Akira, "A new finite element formulation for computational fluid dynamics: II. beyond supg," *Computer Methods in Applied Mechanics and Engineering*, vol. 54, no. 3, pp. 341–355, 1986.
- [21] S. Subramanian and U. Kumar, "Existence of boundary error transverse to the velocity in supg solution of moving conductor problem," in *Numerical Electromagnetic and Multiphysics Modeling and Optimization (NEMO), 2016 IEEE MTT-S International Conference on*. IEEE, 2016, pp. 1–2.
- [22] R. Codina, "A discontinuity-capturing crosswind-dissipation for the finite element solution of the convection-diffusion equation," *Computer Methods in Applied Mechanics and Engineering*, vol. 110, no. 3, pp. 325–342, 1993.
- [23] E. Oñate, F. Zárate, and S. R. Idelsohn, "Finite element formulation for convective-diffusive problems with sharp gradients using finite calculus," *Computer methods in applied mechanics and engineering*, vol. 195, no. 13, pp. 1793–1825, 2006.
- [24] V. John and P. Knobloch, "On spurious oscillations at layers diminishing (sold) methods for convection-diffusion equations: Part i—a review," *Computer Methods in Applied Mechanics and Engineering*, vol. 196, no. 17, pp. 2197–2215, 2007.
- [25] —, "On spurious oscillations at layers diminishing (sold) methods for convection-diffusion equations: Part ii—analysis for p1 and q1 finite elements," *Computer Methods in Applied Mechanics and Engineering*, vol. 197, no. 21, pp. 1997–2014, 2008.
- [26] S. Subramanian and U. Kumar, "Augmenting numerical stability of the galerkin finite element formulation for electromagnetic flowmeter analysis," *IET Science, Measurement & Technology*, vol. 10, no. 4, pp. 288–295, 2016.
- [27] S.-K. Hong and N. Ida, "Modeling of velocity terms in 3d eddy current problems," *IEEE Trans. Magnetics*, vol. 28, no. 2, pp. 1178–1181, 1992.
- [28] J. Shercliff, *The Theory of Electromagnetic Flow-Measurement*, ser. Cambridge Science Classics. Cambridge University Press, 1987.
- [29] P. P. Silvester and R. L. Ferrari, *Finite elements for electrical engineers*. Cambridge university press, 1996.
- [30] G. Mur, "Edge elements, their advantages and their disadvantages," *IEEE transactions on magnetics*, vol. 30, no. 5, pp. 3552–3557, 1994.
- [31] —, "The fallacy of edge elements," *IEEE Transactions on Magnetics*, vol. 34, no. 5, pp. 3244–3247, 1998.
- [32] S. Subramanian and U. Kumar, "Stable galerkin finite-element scheme for the simulation of problems involving conductors moving rectilinearly in magnetic fields," *IET Science, Measurement & Technology*, vol. 10, no. 8, pp. 952–962, 2016.
- [33] T.-P. Fries and H. G. Matthies, "A review of petrov-galerkin stabilization approaches and an extension to meshfree methods," *Technische Universität Braunschweig, Brunswick*, 2004.
- [34] T. J. Hughes, "Multiscale phenomena: Green's functions, the dirichlet-to-neumann formulation, subgrid scale models, bubbles and the origins of stabilized methods," *Computer methods in applied mechanics and engineering*, vol. 127, no. 1, pp. 387–401, 1995.
- [35] A. N. Brooks and T. J. Hughes, "Streamline upwind/ Petrov-galerkin formulations for convection dominated flows with particular emphasis on the incompressible navier-stokes equations," *Computer methods in applied mechanics and engineering*, vol. 32, no. 1, pp. 199–259, 1982.



Sethupathy Subramanian received the bachelors degree in electrical and electronics engineering from Anna University, Chennai, India, in 2009. He received the masters and doctorate degrees in electrical engineering from Indian Institute of Science, Bangalore, India in 2011 and 2017 respectively. He is currently pursuing his graduate research at the Department of Physics, University of Notre Dame, USA.

His research interests, pertinent to electrical engineering, include computational electromagnetics, numerical stability, finite element and edge element methods.



Udaya Kumar (Senior Member, IEEE) received the bachelor's degree in electrical engineering from Bangalore University, Bangalore, India, in 1989, and the M.E. and Ph.D. degrees in high-voltage engineering from the Indian Institute of Science, Bangalore, India, in 1991 and 1998, respectively.

He is currently a Professor with the High Voltage Laboratory, Department of Electrical Engineering, Indian Institute of Science. He is an Associate Editor of IEEE Transactions on Power Delivery & IET High Voltage.



Sujata Bhowmick received the B.E. degree in electrical engineering from IIST, Shibpur, India, in 2006, and the M.E. degree in electrical engineering from the Indian Institute of Science, Bangalore, India, in 2011. She received the Ph.D. degree from the Department of Electronic Systems Engineering, Indian Institute of Science, Bangalore, India, in 2019.

Her current research interests include power electronics for renewable resources, single-phase grid-connected power converters, computational electromagnetics, finite element and edge element methods.